Regular Article

MYELOID NEOPLASIA

Genetic dissection of leukemia-associated IDH1 and IDH2 mutants and D-2-hydroxyglutarate in *Drosophila*

Zachary J. Reitman,[1,2] Sergey A. Sinenko,[3] Eric P. Spana,[4] and Hai Yan[1,2]

[1]The Preston Robert Tisch Brain Tumor Center, [2]Department of Pathology, and [3]Department of Pharmacology and Cancer Biology, Duke University Medical Center, Durham, NC; and [4]Department of Biology, Duke University, Durham, NC

Key Points

- Homologs to cancer-derived IDH1 and IDH2 mutants produce D-2HG and drive expansion of *Drosophila* blood cells.
- In flies, mutant Idh interacts with genes that regulate reduced nicotinamide adenine dinucleotide phosphate, reactive oxygen species, and apoptosis.

Gain-of-function mutations in nicotinamide adenine dinucleotide phosphate–dependent isocitrate dehydrogenase (IDH)1 and IDH2 frequently arise in human leukemias and other cancers and produce high levels of D-2-hydroxyglutarate (D-2HG). We expressed the R195H mutant of *Drosophila* Idh (CG7176), which is equivalent to the human cancer-associated IDH1-R132H mutant, in fly tissues using the UAS-Gal4 binary expression system. Idh-R195H caused a >25-fold elevation of D-2HG when expressed ubiquitously in flies. Expression of mutant Idh in larval blood cells (hemocytes) resulted in higher numbers of circulating blood cells. Mutant Idh expression in fly neurons resulted in neurologic and wing-expansion defects, and these phenotypes were rescued by genetic modulation of superoxide dismutase 2, p53, and apoptotic caspase cascade mediators. Idh-R163Q, which is homologous to the common leukemia-associated IDH2-R140Q mutant, resulted in moderately elevated D-2HG and milder phenotypes. We identified the fly homolog of D-2-hydroxyglutaric acid dehydrogenase (CG3835), which metabolizes D-2HG, and showed that coexpression of this enzyme with mutant Idh abolishes mutant Idh-associated phenotypes. These results provide a flexible model system to interrogate a cancer-related genetic and metabolic pathway and offer insights into the impact of IDH mutation and D-2HG on metazoan tissues.
(*Blood*. 2015;125(2):336-345)

Introduction

Somatic, gain-of-function mutations in nicotinamide adenine dinucleotide phosphate ($NADP^+$)-dependent isocitrate dehydrogenase (IDH)1 and IDH2 occur frequently in acute myeloid leukemias, myelodysplastic syndromes, angioimmunoblastic T-cell lymphomas, brain tumors, and other cancers.[1-9] The mutations occur at the conserved active-site residues of Arg132 in IDH1, or Arg140 and Arg172 in IDH2. When mutated, IDH1 and IDH2 lose their normal function to convert isocitrate to α-ketoglutarate and acquire a gain of function to convert α-ketoglutarate to D-2-hydroxyglutarate (D-2HG).[10] D-2HG accumulates to ~100-fold higher levels in IDH-mutated cancer tissues.[10,11] D-2HG inhibits Fe(II)-α-ketoglutarate-dependent dioxygenases, including histone demethylases, DNA hydroxymethyltransferases, and collagen proline hydroxylases.[12,13] Inhibition of these dioxygenase enzymes leads to histone lysine hypermethylation, DNA hypermethylation, and collagen dysfunction in mammalian tissues expressing mutated IDH1 or IDH2.[5,14-16] IDH mutations can also sensitize cells to reactive oxygen species (ROS) induction, possibly because mutant IDH consumes reduced NADP (NADPH), a cofactor important for scavenging intracellular ROS.[17] Targeting mutated IDH1 or IDH2 to mouse hematopoietic progenitors results in an increased number of these progenitors and can cooperate with other aberrations to drive acute leukemias.[5,14,18-20] Targeting mutant IDH1 or IDH2 to the mouse central nervous system (CNS) results in neurodegeneration or perturbed basement membrane function, without evidence yet that it can drive tumorigenesis in the CNS.[14,21]

IDH mutations are being pursued as therapeutic targets.[10,22-24] However, the mechanisms by which IDH mutants contribute to cancer pathogenesis remain only partially understood. One hurdle to elucidating the role of IDH mutations in cancer is that D-2HG produced by IDH mutations inhibits a large family of enzymes with broad downstream effects, making the relative contribution of any single downstream genetic pathway to tumor pathogenesis unclear. Other hurdles include the lack of model systems amenable to large genetic screens to identify additional therapeutic susceptibilities for IDH-mutated cancers, as well as a poor general understanding of the fundamental role of D-2HG in cellular metabolism.[25] Much insight on cancer-associated genes has been gleaned from research of their homologs in *Drosophila*.[26-28] Human cancer genes, or their *Drosophila* orthologs, can cause cancer-like phenotypes in flies, including increased proliferation, impaired apoptosis, altered migration, growth in inappropriate

Submitted May 23, 2014; accepted October 28, 2014. Prepublished online as *Blood* First Edition paper, November 14, 2014; DOI 10.1182/blood-2014-05-577940.

The data reported in this article have been deposited in the Gene Expression Omnibus database (accession number GSE62008).

The online version of this article contains a data supplement.

The publication costs of this article were defrayed in part by page charge payment. Therefore, and solely to indicate this fact, this article is hereby marked "advertisement" in accordance with 18 USC section 1734.

Table 1. Phenotypes associated with targeted Idh-R195H expression

Promoter	Genotype	Lineage	Phenotype (25°C)
Tubulin	w*;P{a-tubulin84B-GAL4}/TM3,Sb	Ubiquitous (strong promoter)	e17 lethal
Ubiquitin	w*; P{Ubi-GAL4}2/CyO	Ubiquitous (weaker promoter)	Pupa lethal
Actin5c	w*;P{Act5C-GAL4}/CyO	Ubiquitous (++gut expression)	Larva/pupa lethal
Hsp70 (1h 37C heat-shock)	w*; P{GAL4-Hsp70.PB}89-2-1	Heat-shock ubiquitous	—
Elav	P{w[+mW.hs]=GawB}Elav[C155]	Neurons	Wing expansion, severe behavioral defect
Nubbin	P{UAS-Dcr-2.D}1; P{GawB}nubbin-AC-62	Wing disc (neurons?)	Wing expansion, behavioral defect
CCAP	y[1] w[67c23]; P{w[+mC] y[+mDint2]=EPgy2} CCAP[EY15558]	Bursicon-secreting neurons	Wing expansion defect
Inscuteable	w*; P{GawB}insc[Mz1407]	Neuroblasts	—
Repo	w[1118]; P{w[+m*]=GAL4}repo/TM3, Sb[1]	Glia	—
Glial cells missing	y[1] w*; P{gcm-GAL4.U}/CyO	Embryonic glia and hemocytes	—
Glass multiple reporter	w[1118]; P{GMR-GAL4.w[-]}2/CyO	Differentiated eye	—
Eyeless	w[*]; P{w[+m*]=GAL4-ey.H}3-8	Eye, throughout development	—
Hemolectin	w[1118]; P{w[+mC]=Hml-GAL4.Δ}2, P{w[+mC]=UAS-2xEGFP}AH2	Plasmatocytes, crystal cells	Rare melanotic masses
Unpaired	P{upd3-GAL4}	Hematocytes/ubiquitous	Possible developmental delay
E22c	y1 w*; P{en2.4-GAL4}e22c; P{tGPH}4/TM3, Ser1	Muscle/hematocytes	Eclosion defect, motor defect
Beadex	P{GawB}Bx[MS1096]; P{UAS-Dcr-2.D}2	Dorsal wing disc	Curly wings (100%), ectopic wing vein (50%)
Salm	P{UAS-Dcr-2.D}1; P{GawB}salm[LP39]	Wing disc, ubiquitous	Multistage lethal
Bs	P{UAS-Dcr-2.D}1; P{bs-GAL4.Term}G1	Wing disc	Wing margin scalloping
bbg	P{UAS-Dcr-2.D}1; P{GawB}bbg[C96]	Dorsal-ventral margin of wing disc	—
Pnr	P{UAS-Dcr-2.D}1; P{GawB}pnr[MD237]	Hemocytes, dorsal cells along length of fly	—
Serpent	P{srp-GAL4}	Embryonic hemocyte, lymph gland	—
Lozenge	P{w+mC = UAS − mCD8::GFP.L}LL4,y1w* P{w+mW.hs = GawB}lz−Gal4	Crystal cells	—

All phenotypes listed were caused by multiple independent insertions of the Idh-R195H construct but were not elicited by the Idh-WT construct. CCAP, crustacean cardioactive peptide. —, indicates no gross phenotype was observed.

environments, and deregulated differentiation.[29-31] Also, *Drosophila* has a primitive hematopoietic system that shares conserved gene regulatory and signaling pathway features with human hematopoiesis.[32-35] In fact, introduction of oncogenes such as AML1-ETO fusion and the hyperactive fly homolog of JAK2 can also block differentiation or stimulate proliferation of *Drosophila* blood cells.[36-41] We reasoned that *Drosophila* could provide insight into the function of IDH mutations from human cancer and could be used as a model to reveal genetic interactions that mutant IDH and D-2HG depend on to drive their biological phenotypes.

Drosophila contains a single $NADP^+$-dependent IDH called Idh (CG7176; note the lower-case "dh" for fly Idh, in contrast to all capital letters for human IDH1 and IDH2). Idh is 73% and 66% identical at the protein level to human IDH1 and IDH2, respectively (see supplemental Figure 1 on the *Blood* Web site). Idh has NADP-IDH activity, which is present nearly ubiquitously throughout the fly, and localizes to both the cytosol and mitochondria.[42,43] No *Drosophila* models for IDH1-mutated cancer or deregulated D-2HG metabolism have yet been described. Here, we express a cancer-homologous Idh mutant in various fly tissues and find that it causes durable blood and CNS phenotypes by upregulating D-2HG levels. We show that these phenotypes are modified by alterations in a variety of genetic pathways.

Materials and methods

Transgenic Idh and D2hgdh flies

The 1437-bp translated region of Idh transcript CG7176-RK and the 1602-bp translated region of D-2-hydroxyglutaric acid dehydrogenase (D2hgdh) transcript CG3835-A were amplified by polymerase chain reaction from a pupa complementary DNA library without 3′ STOP codons and cloned into pTWF (Gateway II collection), which includes mini-white ([+mC]) eye color marker, 5′ *UASt* for Gal4-driven expression, C-terminal FLAG, SV40 terminator, and flanking P-element insertion sites. Mutagenesis was performed using the QuikChange Site-Directed Mutagenesis Kit (Agilent, Santa Clara, CA).

Stable stocks with *UAS*-transgenes were generated using standard P-element transformation.[44] Injection into *w1118* embryos was performed with Duke Model System Genomics (Duke Center for Genomic and Computational Biology, Durham, NC). Male and virgin P0 hatchlings were crossed to 3 *w* virgins or males, respectively. F1 offspring were screened for males with colored eyes, reflecting inheritance of the transgenic construct. Those on chromosomes 2 or 3 were balanced and homozygosed when possible. *UAS*-Idh-R195H and *UAS*-Idh-WT fly cultures have been deposited to the Bloomington Drosophila Stock Center.

Additional fly lines

The genotypes for additional fly lines are listed in Table 1, supplemental Tables 2 and 3, or the figure legends. Lines were obtained from the Bloomington Drosophila Stock Center unless otherwise indicated. *Gcm*-Gal4 was from V. Hartenstein. MalDH hypermorph/TM8 M89, MalDH KD/TM8 M9, MalDH-WT M3, and *UAS*-G6PDH were used previously,[45] as was *UAS*-AML1-ETO/TM3,Sb.[36] *UAS*-EGFR-λ was from T. Schupach. The *hemolectin* driver was *hml*Δ-Gal4.[46] *hopscotch*-Tum-l/CyO, *Srp*-Gal4, *hml*Δ-Gal4, *Pnr*-Gal4/TM6b, *E33c*-Gal4, and *Lz*-Gal4 were from B. Mathey-Prevot. *Actin5c*-Gal4, *UAS*-CD8GFP/TM3, and other complex lines were derived by standard recombination. Experiments were carried out at 25°C unless otherwise specified.

D-2HG quantification

To compare whole-animal D-2HG production associated with different transgenes, D-2HG was measured in transgenic animals containing *Actin5c*-Gal4 and *UAS*-(transgene of interest) grown at 25°C and collected

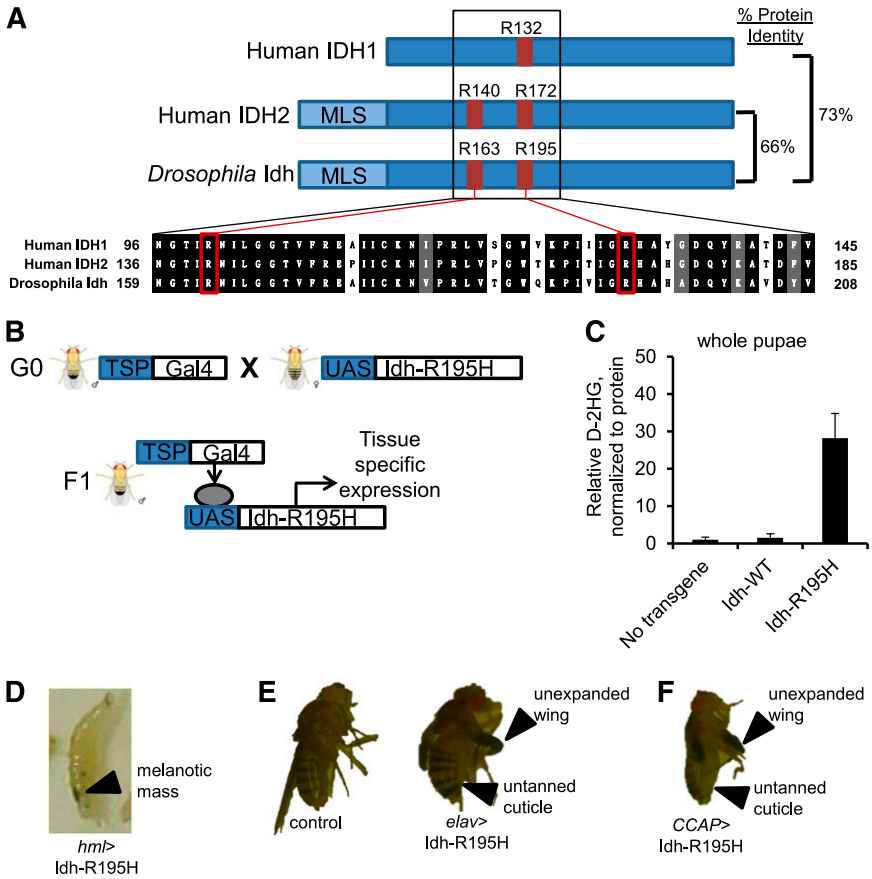

Figure 1. Tissue-specific expression of Idh-R195H, the *Drosophila* homolog to IDH1-R132H, results in D-2HG production. (A) Homology between human IDH1 (GI: 49168486), human IDH2 (GI: 28178832), and *Drosophila* Idh (CG7176-RK translated region). Human cancer hotspots, including IDH1 R132, IDH2 R140, and IDH2 R172, are shown in red with homologous residues in *Drosophila* Idh. (B) The UAS/Gal4 binary expression system to express Idh-R195H in targeted tissue lineages. (C) D-2HG in whole pupae, with expression of the indicated transgene driven by the *Actin5c* driver. Pupae were F1 from the cross of *Actin5c*-Gal4 and *UAS*-transgene flies. Data are expressed as mean ± standard deviation (n = 3). (D) Third instar wandering larva with Idh-R195H expressed in hemocytes demonstrating melanotic mass, genotype *hml*-Gal4, *UAS*-GFP/+; *UAS*-Idh-R195H/+ (*hml*>Idh-R195H). (E) Panneuronal expression of Idh-R195H using the *Elav* promoter leads to eclosion defect, locomotor defect, and early lethality. Adult *Elav*-Gal4/+; *UAS*-Idh-R195H/+ fly exhibiting a wing-expansion defect (top arrow) and cuticle-tanning defect (bottom arrow) is shown. (F) Flies expressing Idh-R195H in CCAP neurons demonstrate wing expansion defect (top arrow) and cuticle-tanning defect (bottom arrow) without obvious locomotor defects. Genotype: *CCAP*-Gal4/+; *UAS*-Idh-R195H/+. Flies were visualized on a Leica Kombistereo microscope, original magnification ×10. MLS, mitochondria localization signal; TSP, tissue-specific promoter.

72 hours after puparium formation. The rationale for examining the pupae life stage, the cross scheme, and the extraction protocol is detailed in the supplemental Methods. D-2HG quantification by liquid chromatography/tandem mass spectrometry was described previously.[47] D-2HG levels were normalized to homogenate protein concentration and reported relative to the no-*UAS*-transgene control from the same experiment.

Immunofluorescence and immunoblots

For primary antibody staining, rabbit anti–green fluorescent protein (GFP) was used at 1:100 (Life Technologies). Rabbit anti-FLAG was used at 1:100 (OriGene Technologies, Rockville, MD). Rabbit anti-L1 (1:100), anti-C4 (1:100), and anti-P1a/b (1:30) were a gift from I. Ando.[48-51] Secondary antibodies with conjugated reporters were used to visualize tissues. Alexa 488-conjugated anti-mouse immunoglobulin G or Alexa 594-conjugated goat anti-rabbit immunoglobulin G (Molecular Probes, Eugene, OR) were applied at 1:200, or rhodamine-conjugated goat anti-mouse and fluorescein isothiocyanate–conjugated goat anti-rabbit were used at 1:10 (Life Technologies). VectaShield with 4′,6-diamidino-2-phenylindole (Vector Laboratories, Burlingame, CA) was used as a mounting medium. Primary antibodies were omitted in negative controls. Immunoblots were performed using anti-FLAG as above with a horseradish peroxidase–linked secondary antibody and SuperSignal West Dura Chemiluminescent Substrate (Thermo Scientific, Waltham, MA).

Hemocyte counting

Circulating hemocytes were collected from 3 wandering third instar larvae in a droplet of 30 μL of Schneider's *Drosophila* medium (Life Technologies) by carefully piercing and opening the rear dorsal aspect of segments 11-13 with number 5 forceps and by gently shaking circulating hemocytes into the droplet without disturbing the lymph gland. To count hemocytes, 10 μL of this mix were added to a hemocytometer, and GFP+ cells were counted using a fluorescein isothiocyanate filter.

In vivo interaction profiling

Candidates were identified by combining a literature search and homology searches with the Drosophila RNAi Screening Center Integrative Ortholog Prediction Tool (http://www.flyrnai.org/cgi-bin/DRSC_orthologs.pl) as described in the supplemental Methods.[52,53] Fly genes with protein–protein, genetic, gene–transcription factor, and gene–micro RNA interactions with wild-type Idh were identified using the Drosophila Interactions Database[54] (www.droidb.org). Stocks containing constructs to overexpress candidate genes and stocks containing constructs to knock down candidate genes from the Transgenic RNAi Project at Harvard Medical School (http://www.flyrnai.org)[55,56] were selected for screening. Screening was done by mating virgin females from a purebreeding stock containing homozygous Gal4 driver and homozygous *UAS*-Idh-R195H with a purebreeding stock containing the modifying transgene of interest. This cross yielded F1 offspring that have 1 copy each of the Gal4 driver, *UAS*-Idh-R195H, and the genetic modifier of interest.

Gene expression analysis

Twenty-four-hour egg lays were set up with 10 male and 10 female *hml*>+ or *hml*>Idh-R195H adults at 29°C. Wandering third instar larvae were harvested on day 7. Hemocytes from 400 larvae, collected 10 at a time in 100-μL droplets of ice-cold Hank's Balanced Salt Solution, were obtained as described above, spun down gently (300*g* for 5 minutes), and washed. RNA was extracted with the RNeasy kit with DNase treatment (Qiagen, Hilden, Germany). Affymetrix GeneChip Drosophila Genome 2.0 Arrays (18 880 probe sets, >18 500 transcripts) were processed using the Ambion MessageAmp Premier Package and Partek Genomics Suite v6.0 at the Duke Institute for Genome Sciences and Policy Microarray Facility. Data are available at the Gene Expression Omnibus repository (http://www.ncbi.nlm.nih.gov/geo; accession number GSE62008). Pathway analysis was carried out using DAVID Functional Annotation Bioinformatics Analysis (http://david.abcc.ncifcrf.gov/).[57]

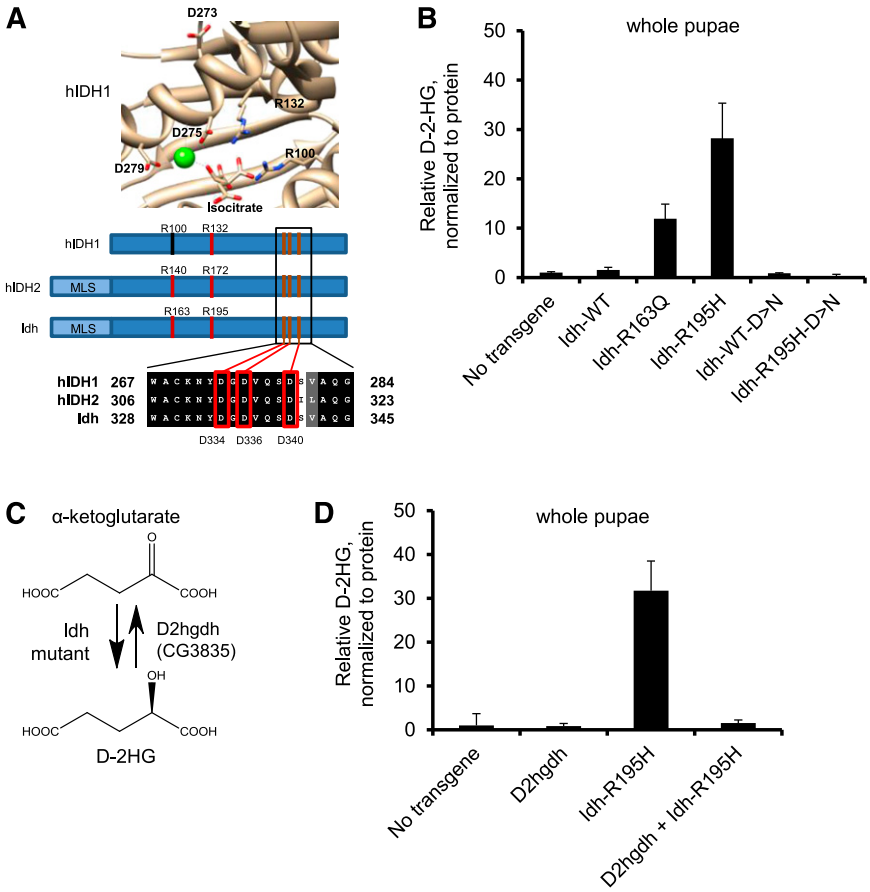

Figure 2. D-2HG mediates mutant Idh phenotypes in *Drosophila*. (A) Structure of active site of human (h) IDH1 (1T0L displayed with UCSF Chimera v1.5; National Institutes of Health)[64,65] with critical metal-binding residues shown, including Asp273, Asp275, and Asp279. Homology analysis shows that Asp334, Asp336, and Asp340 are the homologous residues in fly Idh. (B) D-2HG levels in pupae ubiquitously expressing no transgene, wild-type (WT) Idh, Idh-R163Q, Idh-R195H, and Idh-D>N in which the 3 metal-binding Asp residues are mutated to Asn (D334N-D336N-D340N), and expressing Idh containing the R195H gain-of-function mutation and the D334N-D336N-D340N metal-binding residue mutations (Idh-R195H-D>N). (C) Schematic showing NADPH-linked D-2HG production by Idh mutants, including Idh-R195H. D2HGDH is an FAD-linked enzyme that converts D-2HG to α-ketoglutarate. D2hgdh (CG3835) is a candidate D2HGDH homolog in *Drosophila*. (D) Pupae ubiquitously expressing Idh-R195H, D2hgdh, neither, or both were analyzed for D-2HG. Data are expressed as mean ± standard deviation from 2 replicates and are representative of 3 independent experiments.

Results

Mutant Idh produces D-2HG and elicits blood and brain phenotypes

We identified Arg195 of *Drosophila* Idh as the homologous residue to Arg132 of human IDH1, the most frequently mutated residue of IDH1 in human leukemia (Figure 1A). We used the UAS/Gal4 binary expression system[58] to express Idh-R195H or wild-type Idh with C-terminal FLAG tags in specific fly tissue lineages (Figure 1B). Expression of mutant Idh and other transgenes generated in this study was confirmed by immunoblots showing FLAG-tagged proteins of the appropriate molecular weight in pupae driving expression by the ubiquitous *Actin5c* promoter (supplemental Figure 2). To compare whole-animal D-2HG production associated with Idh-R195H and other transgenes, we developed a liquid chromatography/tandem mass spectrometry–based assay to quantify D-2HG in pupae. Ubiquitous Idh-R195H expression driven by the *Actin5c* promoter was associated with ~30-fold elevated D-2HG in pupae compared with wild-type Idh and no-transgene controls, confirming that Idh-R195H gains the ability to produce D-2HG (Figure 1C).

We surveyed the phenotypes elicited by Idh-R195H when expressing it under control of a panel of 22 tissue-specific drivers (Table 1). Ubiquitous Idh-R195H expression led to lethality at various developmental stages. For instance, the strong ubiquitous *Tubulin* driver led to embryonic lethality, whereas the weaker ubiquitous *Ubiquitin* and *Actin5c* promoters led to lethality at late pupal stages. Broad expression of Idh-R195H in fly blood cells (hemocytes) using the *hemolectin* (*hml*-Gal4)[46] driver resulted in the formation of melanotic masses in third instar larvae (Figure 1D). Melanotic masses (also called melanotic tumors or pseudotumors) arise from hemocytes and can be induced by human oncogenes, infection, or other causes of hemocyte deregulation.[36,37,59,60]

Panneuronal expression of Idh-R195H driven by the *Elav* promoter led to a motor defect accompanied by wing-expansion and cuticle-tanning defects (Figure 1E). When Idh-R195H was expressed in CCAP neurons using the *CCAP* promoter, flies also had a wing-expansion defect and a cuticule-tanning defect with ~50% penetrance (Figure 1F). CCAP is expressed in a group of 12 neurons (the crustacean cardioactive peptide neurons). These neurons secrete bursicon, a hormone that regulates wing expansion and cuticule tanning in early adults,[61] 2 processes that we observed to be disrupted by panneuronal expression of Idh-R195H. Idh-R195H was unable to phenocopy the *Elav/CCAP* phenotypes when expressed in glia (*repo*), [62] embryonic glia (*glial cells missing*), [62] neuroblasts (*inscuteable*), [63] or in eye tissue (*eyeless* or *glass multiple reporter*).

D-2HG production is required for mutant Idh phenotypes

To further explore the connection between D-2HG production and fly phenotypes, we examined a moderate D-2HG-producing Idh mutant and an enzyme-dead Idh mutant that cannot produce D-2HG. We identified Arg163 of Idh as the homologous residue to Arg140 of human IDH2, the most frequently-mutated residue of IDH2 in human leukemia (Figures 1A and 2A). The R163Q mutant also overproduced D-2HG (~10-fold elevated), albeit to a lesser extent than the R195H mutant (Figure 2B). The Idh-R163Q mutant elicited a lower penetrance of melanotic mass formation than the R195H mutant when expressed under control of *hml*-Gal4, and no phenotypes

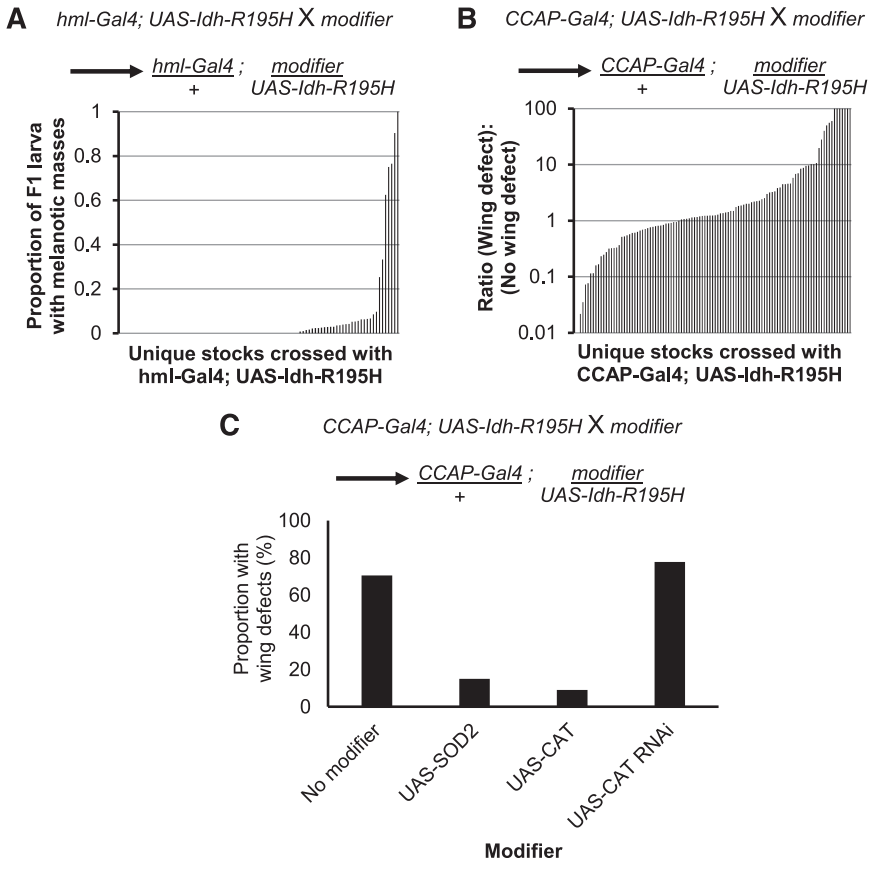

Figure 3. Profiling for genetic interactions with mutant Idh in vivo. (A) Genetic modifiers that enhanced the melanotic mass phenotype induced by mutant Idh were identified by crossing stocks containing a genetic modifier with *hml*-Gal4, *UAS*-2xEGFP; *UAS*-Idh-R195H homozygotes. The resulting offspring were heterozygous for *hml*-Gal4, *UAS*-Idh-R195H, and the genetic modifier. Crosses were carried out at 31°C to enhance the melanotic mass phenotype. Penetrance of melanotic masses is shown for 91 crosses in order of increasing penetrance of the melanotic mass phenotype in the F1 flies. (B) Genetic modifiers that suppressed or enhanced the mutant Idh–induced wing phenotype were identified by crossing stocks containing a genetic modifier with *CCAP*-Gal4, *UAS*-Idh-R195H homozygotes at 25°C. The resulting offspring were heterozygous for *CCAP*-Gal4, *UAS*-Idh-R195H, and the genetic modifier. Penetrance of the wing-expansion defect in 107 crosses is shown in order of increasing penetrance of the wing phenotype. Note the log scale on the y-axis to show the range of phenotype penetrance, with strong suppressors almost completely rescuing the phenotype, and strong enhancers producing almost complete penetrance. (C) Crosses with stocks modifying catalase (CAT) and SOD2. Introduction of SOD2, CAT, or double-stranded RNA targeting CAT to CCAP neurons expressing Idh-R195H. SOD2, superoxide disumutase 2.

when expressed under control of *Tubulin*, *Elav*, and *CCAP* (supplemental Table 1). This finding suggests that higher levels of D-2HG correlate with more penetrant/severe phenotypes. To confirm that enzymatic activity was necessary for mutant Idh to exert biological phenotypes, we generated Idh-R195H that additionally contained mutations in 3 catalytic metal-binding Asp residues to abolish enzymatic activity[66] (Idh-R195H-D334N-D336N-D340N, Figure 2A). This Idh-R195H metal-binding mutant was unable to cause elevated D-2HG levels (Figure 2B). The Idh-R195H metal-binding mutant could not elicit any of the phenotypes of Idh-R195H under control of *hml*, *Tubulin*, *Elav*, or *CCAP* drivers (supplemental Table 1), indicating that catalytic activity is essential for Idh-R195H to cause fly phenotypes.

D2hgdh suppresses mutant Idh phenotypes

We next determined whether clearing D-2HG from the cellular metabolism could rescue flies from mutant Idh-driven phenotypes. To do so, we sought to overexpress D2HGDH, an FAD-linked enzyme that converts D-2HG to α-ketoglutarate, for which a homolog has not yet been reported in flies (Figure 2C). We identified CG3835 as a candidate homolog in *Drosophila* with 51% protein identity to human D2HGDH at the protein level, and named this gene D2hgdh (supplemental Figure 3). Flies were generated to express D2hgdh under UAS/Gal4 control. Coexpression of D2hgdh along with Idh-R195H resulted in 20-fold suppression of D-2HG levels compared with Idh-R195H expression alone (Figure 2D), confirming that D2hgdh encodes a functional D2HGDH enzyme. The severe Idh-R195H-associated *Tubulin*, *Elav*, and *CCAP* phenotypes were completely rescued by coexpression of D2hgdh (supplemental Table 1).

In vivo interaction profiling

To further characterize this fly model of Idh mutation, we tested whether modification of candidate genes could enhance or suppress the blood and CNS phenotypes elicited by mutant Idh. We tested for genetic interactions between Idh-R195H and genes involved in metabolism of substrates such as D-2HG, ROS, and NADPH; other genetic modifications known to cause blood or brain phenotypes in flies; and other pathways (for a full description of our candidate selection strategy, see supplemental Methods). Candidate genes were knocked down using RNA interference (RNAi) stocks from the Transgenic RNAi Project.[67] We also tested whether overexpression of candidate genes modified the phenotypes if gain-of-function alleles were available. We first screened for genetic modifiers that enhanced the penetrance of melanotic masses in wandering larvae expressing Idh-R195H in their hemocytes using the *hml*-Gal4 driver (Figure 3A; supplemental Table 2). Next, we screened for genetic modifiers that enhanced or suppressed the penetrance of the wing-expansion defect of flies expressing Idh-R195H in the CCAP neurons (Figure 3B; supplemental Table 3). Genetic modifiers that enhanced either phenotype were confirmed and also crossed with the Gal4 driver alone to determine whether they synergized with Idh-R195H to enhance the phenotype, or whether they could cause the phenotype independently from Idh-R195H.

The screens revealed that introduction of the ROS-scavenging genes catalase or superoxide dismutase 2 (SOD2) suppressed the wing-expansion defect (Figure 3C). Conversely, knockdown of catalase with RNAi slightly enhanced the wing-expansion phenotype. Additional enhancers identified in these screens that were confirmed and tested with driver alone are shown in supplemental

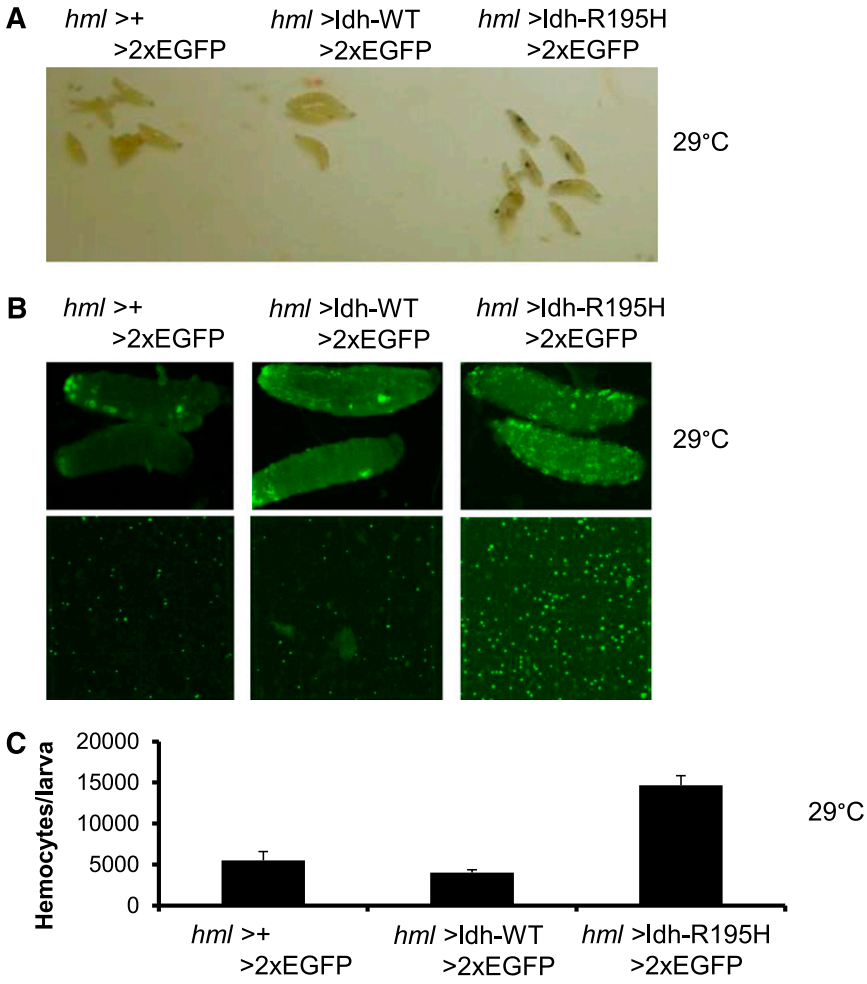

Figure 4. Blood cell proliferation driven by mutant Idh. (A) Melanotic masses in third instar larvae from *hml*-Gal4, *UAS*-2xEGFP (*hml*>+), *hml*-Gal4, *UAS*-2xEGFP; *UAS*-Idh-WT [2;3] (*hml*>Idh-WT), and *hml*-Gal4, *UAS*-2xEGFP; *UAS*-Idh-R195H [2;3] (*hml*>Idh-R195H). (B) Circulating GFP-positive hemocytes in *hml*>+, *hml*>Idh-WT, and *hml*>Idh-R195H larvae. (C) Quantitation of circulating hemocytes in *hml*>Idh-R195H larvae (n = 3; data are expressed as mean ± standard deviation). *Drosophila* were cultured at 29°C. Samples were visualized using a Nikon TE2000-E phase-contrast inverted epifluorescence microscope with a SensiCamQE camera, original magnification ×10, with MetaMorph, v6.2r6 software.

Figures 4 and 5. These results suggested that ROS plays a role in eliciting phenotypes associated with mutant Idh, leading us to focus our studies on genetic pathways related to ROS signaling. Because hemocyte proliferation and differentiation are regulated by ROS,[36] we next sought to more fully characterize the effect of mutant Idh expression on hemocyte biology.

Mutant Idh expands distinct pools of circulating hemocytes

To further investigate the hemocyte phenotype caused by Idh-R195H, we tested whether increased mutant Idh expression led to a more severe phenotype. A fly stock homozygous for both the *hml*-Gal4 and *UAS*-Idh-R195H transgenes was obtained. When reared at 29°C, ~50% of larvae expressing mutant Idh developed melanotic masses (Figure 4A), and 2.9-fold more circulating hemocytes were present in these larvae compared with controls expressing wild-type Idh or driver alone (Figure 4B-C). GFP and FLAG epitopes were always present in melanotic masses and hemocytes, confirming that the masses derive from proliferating hemocyte precursors expressing mutant Idh (supplemental Figure 6). We next examined hemocyte gene expression patterns associated with Idh-R195H expression by profiling ~18 500 messenger RNA transcripts from circulating larval hemocytes expressing Idh-R195H or driver alone. This analysis revealed enrichment for transcripts associated with enzymatic activity, including a trend for enrichment of transcripts associated with SOD2 activity (P = .08; supplemental Figure 7).

Drosophila exhibits a primitive hematopoietic system in which undifferentiated larval prohemocytes can differentiate into macrophagelike plasmatocytes, crystal cells, or lamellocytes (Figure 5A).[34] Wg is expressed in prohemocytes, which express a relatively low level of *hml*. Wg is also expressed in crystal cells, which strongly express *hml*.[36,68] In larvae expressing Idh-R195H in hemocytes, the pool of Wg+ hemocytes was expanded, and a majority of these Wg+ hemocytes weakly expressed *hml* (Figure 5B), suggesting an expansion of prohemocytes.[68] Nevertheless, a subpopulation of Wg+ cells strongly expressed *hml*, suggesting that crystal cells were also expanded. We confirmed that mature crystal cells were also increased in larvae expressing Idh-R195H using the crystal cell–specific C4 marker (Figure 5C). Idh-R195H expression was also associated with an increase in lamellocytes (L1 marker), which are rare or absent from controls (Figure 5D). These results indicate that mutant Idh increases the production of circulating undifferentiated prohemocytes, as well as mature hemocyte lineages. Expression of Idh-R195H under control of the *unpaired-Gal4* hemocyte driver, which is expressed in hemocytes and other tissues,[69] also resulted in melanotic mass formation in larvae, confirming that Idh-R195H can drive melanotic mass formation from multiple hemocyte lineage drivers. However, Idh-R195H was not associated with obvious circulating hemocyte alterations or melanotic mass formation when expressed in embryonic hemocytes (*serpent*-Gal4),[35] lymph gland cells (*pannier*-Gal4),[70] or crystal cells (*lozenge*-Gal4),[35] which may be due to the strength of these drivers or to the sublineages targeted by these drivers.

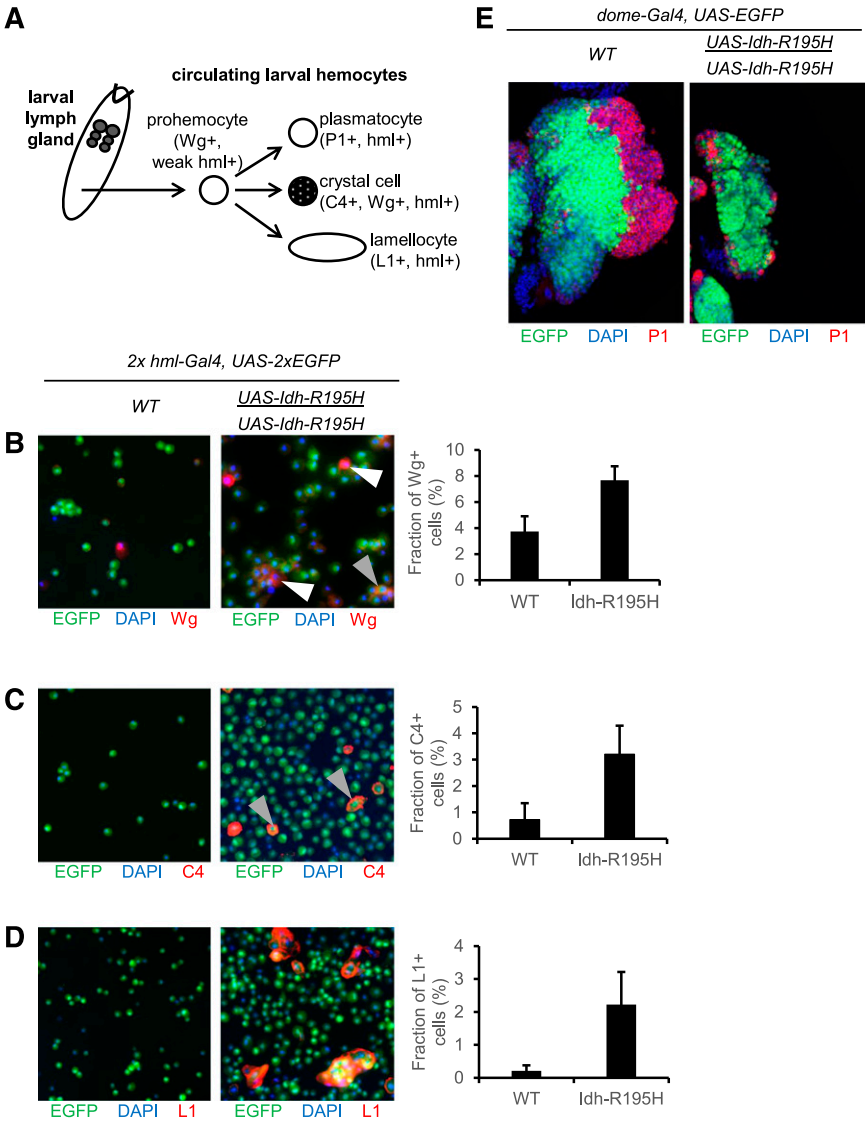

Figure 5. Expansion of circulating hemocyte compartments by mutant Idh. (A) Hemocyte differentiation program in *Drosophila*. Prohemocytes are undifferentiated cells in *Drosophila* that are Wg+.[68] The lymph gland is the organ for hematopoiesis where maintenance and differentiation of prohemocytes occurs in postembryonic *Drosophila*. In larval circulation, prohemocytes can differentiate into crystal cells (C4+), into plasmatocytes (P1+), or under stress into lamellocytes (L1+). (B) Mutant Idh increases Wg+ hemocytes in circulation (red), compared with WT background. Most Wg+ hemocytes had relatively low *hml* expression, as reflected by low enhanced GFP (EGFP) signal, characteristic of prohemocytes (white arrows). Other Wg+ hemocytes strongly expressed *hml*, characteristic of crystal cells (gray arrow).[36,68] (C) Staining of crystal cells in larval circulation (C4+).[51] Mutant Idh induces a slight increase in crystal cell composition. All C4+ cells were strongly *hml*+ (gray arrows). (D) Staining of lamellocytes in larval circulation (L1+). Mutant Idh induces an increase in lamellocyte composition. (E) The third instar larval lymph gland. Hemocyte precursor population or *Dome*+ cells are marked by GFP. Differentiated plasmatocytes of cortical zone are marked by P1,[50,73] shown in red. Mutant Idh expression under control of the lymph gland hemocyte *dome*-Gal4 driver is associated with a lack of differentiated cortical zone plasmatocytes (red) compared with controls. Genotypes for panels B-D: *hml*-Gal4, *UAS*-2xEGFP (control); *hml*-Gal4, *UAS*-2xEGFP; *UAS*-Idh-R195H (Idh mutant). Genotypes for panel E: *dome*-Gal4, *UAS*-EGFP/+ (control); *dome*-Gal4, *UAS*-EGFP/+; *UAS*-Idh-R195H/*UAS*-Idh-R195H (Idh mutant). Data are expressed as mean ± standard deviation for 3 independent groups of animals. Samples were visualized using a Nikon TE2000-E phase-contrast inverted epifluorescence microscope with a SensiCamQE camera, original magnification ×10, with MetaMorph, v6.2r6 software. Wg, *Wingless*.

The lymph gland is the main organ of hematopoiesis in postembryonic *Drosophila*. We next determined the effect of Idh-R195H on the blood precursors of the medullary zone of the lymph gland using the *dome*-Gal4 driver.[33] As with circulating hemocytes, the effect of Idh-R195H expression was dose-dependent, because 2 copies of *UAS*-Idh-R195H with *dome*-Gal4 resulted in a strong effect on lymph gland development (Figure 5E). Idh-R195H expression resulted in smaller lymph glands, a dramatic reduction in the number of *dome*+ cells, and near-absence of differentiated cortical hemocytes. Together, these results indicate that expression of Idh-R195H in *hml*+ differentiating cells promotes growth and/or differentiation of circulating hemocytes, whereas expression of Idh-R195H in lymph gland prohemocytes may limit hemocyte differentiation and even lymph gland development. These findings suggest that Idh-R195H exerts compartment-specific effects on hemocyte development.

Mutant Idh induces p53 activation in *Drosophila* neurons

Our in vivo interaction profiling revealed that overexpression of SOD2 in CCAP neurons expressing mutant Idh can suppress the wing-expansion phenotype. This finding suggests that the Idh-R195H mutant phenotype depends on high levels of ROS. ROS can mediate alternative cell signaling events, leading to programmed cell death[71] and to activation of cellular proproliferative and survival pathways.[72,73] We therefore speculated that Idh-R195H expression was causing apoptosis of *Drosophila* neurons. To test this, we determined whether genetic disruption of the apoptotic pathway would suppress the wing-expansion defect associated with Idh-R195H expression in CCAP neurons. Removing initiator caspase (Dronc) or apoptosis protease activating factor 1 (DARK) using RNAi suppressed the wing-expansion defect (Figure 6A). Also, expression of additional copies of cell death inhibitor DIAP1 suppressed the wing-expansion defect. Importantly, inactivation of p53 almost completely suppressed the Idh-R195H phenotype in CCAP neurons, suggesting that p53 activates the caspase-dependent apoptotic pathway mediated by Dronc and DARK via inactivation of DIAP1.

To further test whether Idh-R195H can enhance apoptosis, we determined whether introduction of Idh-R195H could enhance apoptotic phenotypes driven by expression of Reaper or by inactivation of DIAP1 in the developing eye. Expression of Idh-R195H, but not wild-type Idh, enhanced apoptotic phenotypes associated with Reaper (Figure 6B) and with dsRNA knockdown of DIAP1 (Figure 6C). This finding suggests that mutant Idh leads

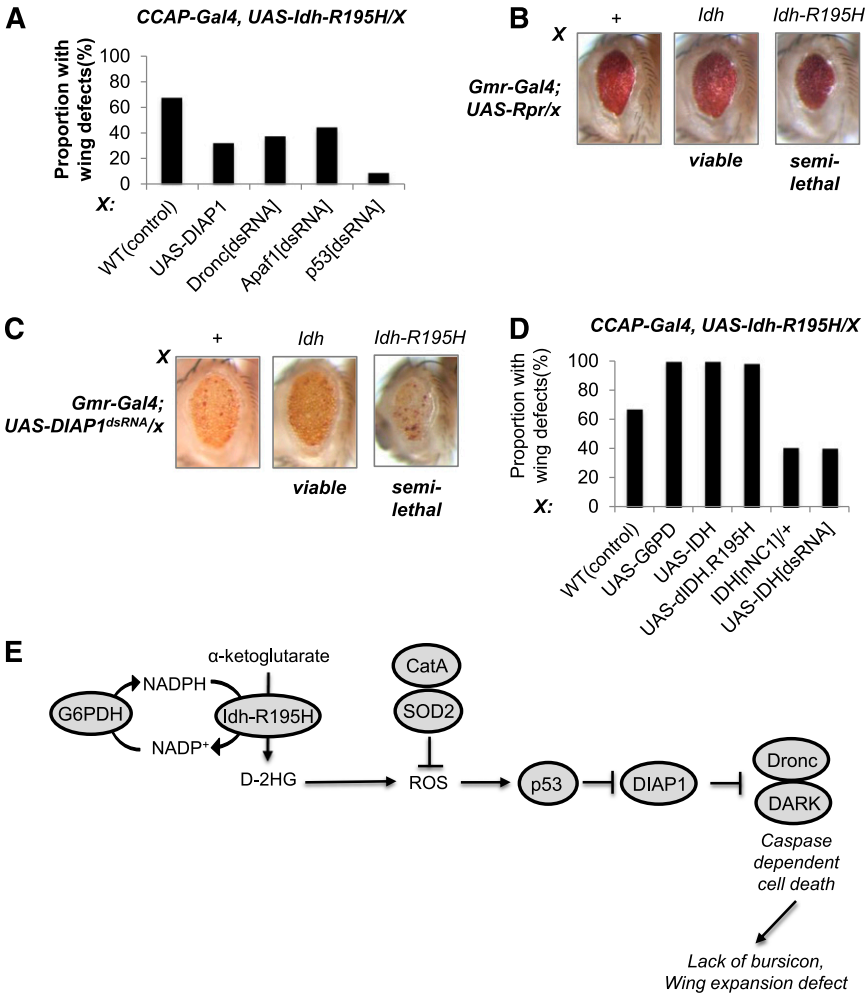

Figure 6. Expression of mutant Idh in the fly CNS. (A) Introduction of genetic elements that modulate caspase-dependent apoptosis genes to CCAP neurons expressing Idh-R195H. (B) Idh-R195H enhances the apoptosis-driven phenotype for developing eye ectopically expressing Reaper (Rpr) under control of the *Gmr*-Gal4 promoter. (C) Idh-R195H enhances the apoptosis-driven phenotype for developing eye cells expressing dsRNA knocking down DIAP1 under control of the *Gmr*-Gal4 promoter. (D) Glucose-6-phosphate dehydrogenase (G6PD or G6PDH) and WT Idh, which are expected to increase the NADPH pool, enhanced the wing-expansion defect caused by expression of Idh-R195H in CCAP neurons. In contrast, alleles expected to lower the pool of NADPH, including a deficiency of Idh and dsRNA against Idh, suppressed the phenotype. (E) Model for Idh-R195H-induced phenotype in the fly CNS. Idh-R195H consumes NADPH and produces D-2HG, leading to ROS formation. This leads to p53-induced caspase-independent cell death. Cell death of CCAP neurons that secrete bursicon to enforce wing expansion leads to a wing-expansion defect. G6PDH and genes that produce NADPH enhance the phenotype. SOD2 scavenges ROS to suppress the phenotype. All crosses were done at 25°C unless otherwise indicated. Genotypes: (A) *CCAP*-Gal4, *UAS*-Idh-R195H/+ (control). *CCAP*-Gal4, *UAS*-Idh-R195H/*UAS*-DIAP1. *CCAP*-Gal4, *UAS*-Idh-R195H/Dronc[dsRNA]. *CCAP*-Gal4, *UAS*-Idh-R195H/Apaf1[dsRNA]. *CCAP*-Gal4, *CCAP*-Gal4, *UAS*-Idh-R195H/p53[dsRNA]. (B) *Gmr*-Gal4/+; *UAS*-Rpr/+. *Gmr*-Gal4/+; *UAS*-Rpr/*UAS*-Idh-WT. *Gmr*-Gal4/+; *UAS*-Rpr/*UAS*-Idh-R195H. (C) *Gmr*-Gal4/+; *UAS*-DIAP1/+. *Gmr*-Gal4/+; *UAS*-DIAP1/*UAS*-Idh-WT. *Gmr*-Gal4/+; *UAS*-DIAP1/*UAS*-Idh-R195H. (D) *CCAP*-Gal4, *UAS*-Idh-R195H/+ (control). *CCAP*-Gal4, *UAS*-Idh-R195H/*UAS*-G6PD. *CCAP*-Gal4, *UAS*-Idh-R195H/*UAS*-Idh-WT. *CCAP*-Gal4, *UAS*-Idh-R195H/+; IDH[nNC1]/+. *CCAP*-Gal4, *UAS*-Idh-R195H/*UAS*-Idh-R195H. IDH[nNC1]/+ indicates a null allele of endogenous Idh.[80] Flies were photographed with a Leica Kombistereo microscope, original magnification ×10. dsRNA, double-stranded DNA.

to elevation of ROS levels that mediate activation of p53 and apoptosis in neurons. We also found that the phenotypes elicited by Idh-R195H were modulated by enzymes that produce NADPH. Overexpression of glucose-6-phosphate dehydrogenase or wild-type Idh in the CCAP neurons led to enhancement of the phenotype (Figure 6D). In contrast, inactivation of endogenous Idh, itself an NADPH producer, suppressed the phenotype. These results indicate that Idh-R195H induces ROS production that enhances p53-dependent, caspase-dependent apoptosis in fly CNS lineages, as depicted in Figure 6E.

Discussion

We used flexible tools to modulate D-2HG in targeted *Drosophila* tissues, including *UAS*-Idh mutants to overproduce D-2HG, and *UAS*-D2hgdh to lower D-2HG. We showed that *Drosophila* exhibits phenotypes when expressing Idh mutants that are equivalent to IDH1 and IDH2 mutants found in different types of human cancer. These phenotypes are driven by D-2HG, which is elevated in flies expressing Idh mutants. The data suggest that mutant Idh expression caused hemocyte differentiation phenotypes analogous to other oncogenes, for instance by altering blood cell differentiation reminiscent of Jak2 (tum-l) mutants,[38,59] and by increasing precursor cells reminiscent of AML1-ETO hemocytes.[36] Expression of mutant Idh in fly blood cells also recapitulated the situation in mouse models of IDH-mutated leukemias, because mutant Idh expression results in expansion of undifferentiated hematopoietic cells and altered blood cell differentiation in fly and mouse systems.[14,18-20]

Because gliomas also frequently harbor IDH mutations, we also sought to model cancerlike phenotypes associated with mutant IDH in the fly brain. However, we were unable to promote cell overgrowth by expressing mutant Idh in fly CNS lineages. The situation is similar for mouse models of IDH-mutated brain tumors, in which so far only neurodegenerative phenotypes have been observed when IDH1 or IDH2 mutants are introduced to the mouse CNS.[14,21] Instead, our results indicate that mutant IDH triggers apoptosis within fly neurons, because modulating p53 or apoptosis cascade genes such as DIAP1, dApaf1/DARK, or Dronc can rescue the defects associated with expression of mutant Idh in CCAP neurons. Importantly, we identified in the genetic screen that scavenging ROS by SOD2 can suppress the Idh mutant phenotype, suggesting that this phenotype is caused by high levels of ROS. We further showed that in the CNS, these high levels of ROS induce a p53-mediated apoptotic cascade rather than prosurvival signaling. In humans, astrocytomas with *IDH1* mutations almost always acquire a *TP53* mutation either concurrently with the *IDH1* mutation or later in their clinical course.[1,74] Our results raise the possibility that the acquisition of *TP53* mutations by these gliomas reflects a selective pressure to suppress a p53-initiated apoptotic cascade that is promoted by *IDH1* mutation.

The level of D-2HG and penetrance of phenotypes was higher for Idh-R195H than for Idh-R163Q. This spectrum of potency for different IDH mutants parallels the situation for human IDH mutants, for which D-2HG is higher for IDH1-R132H (analogous to fly Idh-R195H) compared with IDH2-R140Q (analgous to fly Idh-R163Q) in human cancer tissue and cell lines.[4,75,76] Additionally, our findings that ubiquitous Idh-R195H expression is not compatible with fly development but that ubiquitous Idh-R163Q expression is tolerated into adulthood mirrors the situation for germline and mosaic IDH mutations in humans. Several patients have been described with germline IDH2 Arg140 mutations that result in D-2-hydroxyglutaric aciduria, a rare inborn error of D-2HG metabolism characterized by elevated D-2HG, CNS defects, and a shortened life span.[77] Germline IDH1-R132H mutation has been speculated to be incompatible with human development because it has only been observed in a mosaic distribution, and even then it is associated with severe metaphysical chondromatosis and D-2-hydroxyglutaric aciduria.[78,79]

We developed this *Drosophila* model to enable rapid in vivo assays to identify genetic interactions with mutant IDH, in order to map the molecular pathways by which mutant IDH exerts biological phenotypes and to discover therapeutic susceptibilities of IDH-mutated cancer tissues. We used this system to test whether a focused panel of candidate genes interacted with mutant IDH in the fly. These genetic tools lay the foundation for large *Drosophila* screens to provide new insights into disease pathogenesis and therapeutic susceptibilities for IDH-mutated cancers, as well as for D-2HG-associated disease states such as D-2-hydroxygutaric aciduria. Orthologs of the hits identified in these screens can immediately be tested as therapeutic targets in preclinical mammalian models of human IDH-mutated cancers.

Acknowledgments

The authors thank I. Ando for antibodies; T. Shupbach, V. Hartenstein, and B. Mathey-Prevot for fly lines; S. Kornbluth for laboratory resources; and B. Mathey-Prevot, S. Kornbluth, and C. Marean-Reardon for advice and feedback.

This work was supported by National Institutes of Health, National Cancer Institute grant R01CA140316, American Cancer Society grant RSG-10-126-01-CCE, a Pediatric Brain Tumor Foundation Institute grant, a Voices Against Brain Cancer Foundation grant, a James S. McDonnell Foundation grant, The V Foundation, and an Accelerate Brain Cancer Cure Foundation grant (H.Y.).

Authorship

Contribution: Z.J.R. generated the transgenic flies, designed the experiments, and wrote the manuscript; S.A.S. performed the hemocyte labeling and genetic experiments and assisted with writing the manuscript; E.P.S. provided the reagents; H.Y. provided the funding; and E.P.S. and H.Y. provided critical feedback.

Conflict-of-interest disclosure: The authors declare no competing financial interests.

The current affiliation for Z.J.R. is Department of Medicine, MedStar Union Memorial Hospital, Baltimore, MD.

The current affiliation for S.A.S. is Institute of Cytology, Russian Academy of Science, St. Petersburg, Russia.

Correspondence: Hai Yan, 199 MSRB1, 10 Research Dr, Durham, NC 27710; e-mail: hai.yan@dm.duke.edu.

References

1. Yan H, Parsons DW, Jin G, et al. IDH1 and IDH2 mutations in gliomas. *N Engl J Med.* 2009;360(8):765-773.
2. Schnittger S, Haferlach C, Ulke M, Alpermann T, Kern W, Haferlach T. IDH1 mutations are detected in 6.6% of 1414 AML patients and are associated with intermediate risk karyotype and unfavorable prognosis in adults younger than 60 years and unmutated NPM1 status. *Blood.* 2010;116(25):5486-5496.
3. Abbas S, Lugthart S, Kavelaars FG, et al. Acquired mutations in the genes encoding IDH1 and IDH2 both are recurrent aberrations in acute myeloid leukemia: prevalence and prognostic value. *Blood.* 2010;116(12):2122-2126.
4. Ward PS, Patel J, Wise DR, et al. The common feature of leukemia-associated IDH1 and IDH2 mutations is a neomorphic enzyme activity converting alpha-ketoglutarate to 2-hydroxyglutarate. *Cancer Cell.* 2010;17(3):225-234.
5. Sasaki M, Knobbe CB, Itsumi M, et al. D-2-hydroxyglutarate produced by mutant IDH1 perturbs collagen maturation and basement membrane function. *Genes Dev.* 2012;26(18):2038-2049.
6. Borger DR, Tanabe KK, Fan KC, et al. Frequent mutation of isocitrate dehydrogenase (IDH)1 and IDH2 in cholangiocarcinoma identified through broad-based tumor genotyping. *Oncologist.* 2012;17(1):72-79.
7. Reitman ZJ, Yan H. Isocitrate dehydrogenase 1 and 2 mutations in cancer: alterations at a crossroads of cellular metabolism. *J Natl Cancer Inst.* 2010;102(13):932-941.
8. Amary MF, Damato S, Halai D, et al. Ollier disease and Maffucci syndrome are caused by somatic mosaic mutations of IDH1 and IDH2. *Nat Genet.* 2011;43(12):1262-1265.
9. Pansuriya TC, van Eijk R, d'Adamo P, et al. Somatic mosaic IDH1 and IDH2 mutations are associated with enchondroma and spindle cell hemangioma in Ollier disease and Maffucci syndrome. *Nat Genet.* 2011;43(12):1256-1261.
10. Dang L, White DW, Gross S, et al. Cancer-associated IDH1 mutations produce 2-hydroxyglutarate. *Nature.* 2009;462(7274):739-744.
11. Gross S, Cairns RA, Minden MD, et al. Cancer-associated metabolite 2-hydroxyglutarate accumulates in acute myelogenous leukemia with isocitrate dehydrogenase 1 and 2 mutations. *J Exp Med.* 2010;207(2):339-344.
12. Xu W, Yang H, Liu Y, et al. Oncometabolite 2-hydroxyglutarate is a competitive inhibitor of α-ketoglutarate-dependent dioxygenases. *Cancer Cell.* 2011;19(1):17-30.
13. Chowdhury R, Yeoh KK, Tian YM, et al. The oncometabolite 2-hydroxyglutarate inhibits histone lysine demethylases. *EMBO Rep.* 2011;12(5):463-469.
14. Sasaki M, Knobbe CB, Munger JC, et al. IDH1(R132H) mutation increases murine haematopoietic progenitors and alters epigenetics. *Nature.* 2012;488(7413):656-659.
15. Duncan CG, Barwick BG, Jin G, et al. A heterozygous IDH1R132H/WT mutation induces genome-wide alterations in DNA methylation. *Genome Res.* 2012;22(12):2339-2355.
16. Figueroa ME, Abdel-Wahab O, Lu C, et al. Leukemic IDH1 and IDH2 mutations result in a hypermethylation phenotype, disrupt TET2 function, and impair hematopoietic differentiation. *Cancer Cell.* 2010;18(6):553-567.
17. Mohrenz IV, Antonietti P, Pusch S, et al. Isocitrate dehydrogenase 1 mutant R132H sensitizes glioma cells to BCNU-induced oxidative stress and cell death. *Apoptosis.* 2013;18(11):1416-1425.
18. Chaturvedi A, Araujo Cruz MM, Jyotsana N, et al. Mutant IDH1 promotes leukemogenesis in vivo and can be specifically targeted in human AML. *Blood.* 2013;122(16):2877-2887.
19. Kats LM, Reschke M, Taulli R, et al. Proto-oncogenic role of mutant IDH2 in leukemia initiation and maintenance. *Cell Stem Cell.* 2014;14(3):329-341.
20. Chen C, Liu Y, Lu C, et al. Cancer-associated IDH2 mutants drive an acute myeloid leukemia that is susceptible to Brd4 inhibition. *Genes Dev.* 2013;27(18):1974-1985.
21. Akbay EA, Moslehi J, Christensen CL, et al. D-2-hydroxyglutarate produced by mutant IDH2 causes cardiomyopathy and neurodegeneration in mice. *Genes Dev.* 2014;28(5):479-490.
22. Popovici-Muller J, Saunders JO, Salituro FG, et al. Discovery of the first potent inhibitors of mutant IDH1 that lower tumor 2-HG in vivo. *ACS Med Chem Lett.* 2012;3(10):850-855.
23. Rohle D, Popovici-Muller J, Palaskas N, et al. An inhibitor of mutant IDH1 delays growth and promotes differentiation of glioma cells. *Science.* 2013;340(6132):626-630.
24. Lu C, Venneti S, Akalin A, et al. Induction of sarcomas by mutant IDH2. *Genes Dev.* 2013;27(18):1986-1998.

25. Kranendijk M, Struys EA, Salomons GS, Van der Knaap MS, Jakobs C. Progress in understanding 2-hydroxyglutaric acidurias. *J Inherit Metab Dis.* 2012;35(4):571-587.
26. Brumby AM, Richardson HE. scribble mutants cooperate with oncogenic Ras or Notch to cause neoplastic overgrowth in Drosophila. *EMBO J.* 2003;22(21):5769-5779.
27. Asha H, Nagy I, Kovacs G, Stetson D, Ando I, Dearolf CR. Analysis of Ras-induced overproliferation in Drosophila hemocytes. *Genetics.* 2003;163(1):203-215.
28. Casanova J, Struhl G. The torso receptor localizes as well as transduces the spatial signal specifying terminal body pattern in Drosophila. *Nature.* 1993;362(6416):152-155.
29. Brumby AM, Richardson HE. Using Drosophila melanogaster to map human cancer pathways. *Nat Rev Cancer.* 2005;5(8):626-639.
30. Vidal M, Cagan RL. Drosophila models for cancer research. *Curr Opin Genet Dev.* 2006;16(1):10-16.
31. Miles WO, Dyson NJ, Walker JA. Modeling tumor invasion and metastasis in Drosophila. *Dis Model Mech.* 2011;4(6):753-761.
32. Mathey-Prevot B, Perrimon N. Mammalian and Drosophila blood: JAK of all trades? *Cell.* 1998; 92(6):697-700.
33. Jung SH, Evans CJ, Uemura C, Banerjee U. The Drosophila lymph gland as a developmental model of hematopoiesis. *Development.* 2005; 132(11):2521-2533.
34. Crozatier M, Meister M. Drosophila haematopoiesis. *Cell Microbiol.* 2007;9(5): 1117-1126.
35. Lebestky T, Chang T, Hartenstein V, Banerjee U. Specification of Drosophila hematopoietic lineage by conserved transcription factors. *Science.* 2000; 288(5463):146-149.
36. Sinenko SA, Hung T, Moroz T, et al. Genetic manipulation of AML1-ETO-induced expansion of hematopoietic precursors in a Drosophila model. *Blood.* 2010;116(22):4612-4620.
37. Osman D, Gobert V, Ponthan F, Heidenreich O, Haenlin M, Waltzer L. A Drosophila model identifies calpains as modulators of the human leukemogenic fusion protein AML1-ETO. *Proc Natl Acad Sci USA.* 2009;106(29):12043-12048.
38. Luo H, Hanratty WP, Dearolf CR. An amino acid substitution in the Drosophila hopTum-l Jak kinase causes leukemia-like hematopoietic defects. *EMBO J.* 1995;14(7):1412-1420.
39. Luo H, Rose PE, Roberts TM, Dearolf CR. The Hopscotch Jak kinase requires the Raf pathway to promote blood cell activation and differentiation in Drosophila. *Mol Genet Genomics.* 2002;267(1): 57-63.
40. Agaisse H, Petersen UM, Boutros M, Mathey-Prevot B, Perrimon N. Signaling role of hemocytes in Drosophila JAK/STAT-dependent response to septic injury. *Dev Cell.* 2003;5(3):441-450.
41. Harrison DA, Binari R, Nahreini TS, Gilman M, Perrimon N. Activation of a Drosophila Janus kinase (JAK) causes hematopoietic neoplasia and developmental defects. *EMBO J.* 1995;14(12): 2857-2865.
42. Fox DJ, Conscience-Egli M, Abächerli E. The soluble citric acid cycle enzymes of Drosophila melanogaster. II. Tissue and intracellular distribution of aconitase and NADP-dependent isocitrate dehydrogenase. *Biochem Genet.* 1972;7(2):163-175.
43. Fox DJ. The soluble citric acid cycle enzymes of Drosophila melanogaster. I. Genetics and ontogeny of NADP-linked isocitrate dehydrogenase. *Biochem Genet.* 1971;5(1):69-80.
44. Spradling AC, Rubin GM. Transposition of cloned P elements into Drosophila germ line chromosomes. *Science.* 1982;218(4570):341-347.
45. Yang CS, Thomenius MJ, Gan EC, et al. Metabolic regulation of Drosophila apoptosis through inhibitory phosphorylation of Dronc. *EMBO J.* 2010;29(18):3196-3207.
46. Sinenko SA, Mathey-Prevot B. Increased expression of Drosophila tetraspanin, Tsp68C, suppresses the abnormal proliferation of ytr-deficient and Ras/Raf-activated hemocytes. *Oncogene.* 2004;23(56):9120-9128.
47. Jin G, Reitman ZJ, Spasojevic I, et al. 2-hydroxyglutarate production, but not dominant negative function, is conferred by glioma-derived NADP-dependent isocitrate dehydrogenase mutations. *PLoS ONE.* 2011;6(2):e16812.
48. Kurucz E, Zettervall CJ, Sinka R, et al. Hemese, a hemocyte-specific transmembrane protein, affects the cellular immune response in Drosophila. *Proc Natl Acad Sci USA.* 2003;100(5): 2622-2627.
49. Honti V, Kurucz E, Csordás G, Laurinyecz B, Márkus R, Andó I. In vivo detection of lamellocytes in Drosophila melanogaster. *Immunol Lett.* 2009;126(1-2):83-84.
50. Kurucz E, Márkus R, Zsámboki J, et al. Nimrod, a putative phagocytosis receptor with EGF repeats in Drosophila plasmatocytes. *Curr Biol.* 2007;17(7):649-654.
51. Kurucz E, Váczi B, Márkus R, et al. Definition of Drosophila hemocyte subsets by cell-type specific antigens. *Acta Biol Hung.* 2007;58(Suppl 1):95-111.
52. Klose RJ, Zhang Y. Regulation of histone methylation by demethylimination and demethylation. *Nat Rev Mol Cell Biol.* 2007;8(4): 307-318.
53. Secombe J, Li L, Carlos L, Eisenman RN. The Trithorax group protein Lid is a trimethyl histone H3K4 demethylase required for dMyc-induced cell growth. *Genes Dev.* 2007;21(5):537-551.
54. Murali T, Pacifico S, Yu J, Guest S, Roberts GG III, Finley RL Jr. DroID 2011: a comprehensive, integrated resource for protein, transcription factor, RNA and gene interactions for Drosophila. *Nucleic Acids Res.* 2011;39(Suppl 1):D736-D743.
55. Ni JQ, Liu LP, Binari R, et al. A Drosophila resource of transgenic RNAi lines for neurogenetics. *Genetics.* 2009;182(4): 1089-1100.
56. Ni JQ, Zhou R, Czech B, et al. A genome-scale shRNA resource for transgenic RNAi in Drosophila. *Nat Methods.* 2011;8(5):405-407.
57. Fang YP, Huang YB, Wu PC, Tsai YH. Topical delivery of 5-aminolevulinic acid-encapsulated ethosomes in a hyperproliferative skin animal model using the CLSM technique to evaluate the penetration behavior. *Eur J Pharm Biopharm.* 2009;73(3):391-398.
58. Elliott DA, Brand AH. The GAL4 system : a versatile system for the expression of genes. *Methods Mol Biol.* 2008;420:79-95.
59. Luo H, Rose P, Barber D, et al. Mutation in the Jak kinase JH2 domain hyperactivates Drosophila and mammalian Jak-Stat pathways. *Mol Cell Biol.* 1997;17(3):1562-1571.
60. Minakhina S, Steward R. Melanotic mutants in Drosophila: pathways and phenotypes. *Genetics.* 2006;174(1):253-263.
61. Peabody NC, Pohl JB, Diao F, et al. Characterization of the decision network for wing expansion in Drosophila using targeted expression of the TRPM8 channel. *J Neurosci.* 2009;29(11):3343-3353.
62. Jones BW, Abeysekera M, Galinska J, Jolicoeur EM. Transcriptional control of glial and blood cell development in Drosophila: cis-regulatory elements of glial cells missing. *Dev Biol.* 2004; 266(2):374-387.
63. Li P, Yang X, Wasser M, Cai Y, Chia W. Inscuteable and Staufen mediate asymmetric localization and segregation of prospero RNA during Drosophila neuroblast cell divisions. *Cell.* 1997;90(3):437-447.
64. Xu X, Zhao J, Xu Z, et al. Structures of human cytosolic NADP-dependent isocitrate dehydrogenase reveal a novel self-regulatory mechanism of activity. *J Biol Chem.* 2004; 279(32):33946-33957.
65. Pettersen EF, Goddard TD, Huang CC, et al. UCSF Chimera—a visualization system for exploratory research and analysis. *J Comput Chem.* 2004;25(13):1605-1612.
66. Koivunen P, Lee S, Duncan CG, et al. Transformation by the (R)-enantiomer of 2-hydroxyglutarate linked to EGLN activation. *Nature.* 2012;483(7390):484-488.
67. Dietzl G, Chen D, Schnorrer F, et al. A genome-wide transgenic RNAi library for conditional gene inactivation in Drosophila. *Nature.* 2007; 448(7150):151-156.
68. Sinenko SA, Mandal L, Martinez-Agosto JA, Banerjee U. Dual role of wingless signaling in stem-like hematopoietic precursor maintenance in Drosophila. *Dev Cell.* 2009;16(5):756-763.
69. Harrison DA, McCoon PE, Binari R, Gilman M, Perrimon N. Drosophila unpaired encodes a secreted protein that activates the JAK signaling pathway. *Genes Dev.* 1998;12(20):3252-3263.
70. Minakhina S, Tan W, Steward R. JAK/STAT and the GATA factor Pannier control hemocyte maturation and differentiation in Drosophila. *Dev Biol.* 2011;352(2):308-316.
71. Giorgio M, Migliaccio E, Orsini F, et al. Electron transfer between cytochrome c and p66Shc generates reactive oxygen species that trigger mitochondrial apoptosis. *Cell.* 2005;122(2): 221-233.
72. Sinenko SA, Shim J, Banerjee U. Oxidative stress in the haematopoietic niche regulates the cellular immune response in Drosophila. *EMBO Rep.* 2012;13(1):83-89.
73. Owusu-Ansah E, Banerjee U. Reactive oxygen species prime Drosophila haematopoietic progenitors for differentiation. *Nature.* 2009; 461(7263):537-541.
74. Watanabe T, Nobusawa S, Kleihues P, Ohgaki H. IDH1 mutations are early events in the development of astrocytomas and oligodendrogliomas. *Am J Pathol.* 2009;174(4):1149-1153.
75. Ward PS, Lu C, Cross JR, et al. The potential for isocitrate dehydrogenase mutations to produce 2-hydroxyglutarate depends on allele specificity and subcellular compartmentalization. *J Biol Chem.* 2013;288(6):3804-3815.
76. Grassian AR, Lin F, Barrett R, et al. Isocitrate dehydrogenase (IDH) mutations promote a reversible ZEB1/microRNA (miR)-200-dependent epithelial-mesenchymal transition (EMT). *J Biol Chem.* 2012;287(50):42180-42194.
77. Kranendijk M, Struys EA, van Schaftingen E, et al. IDH2 mutations in patients with D-2-hydroxyglutaric aciduria. *Science.* 2010; 330(6002):336.
78. Vissers LE, Fano V, Martinelli D, et al. Whole-exome sequencing detects somatic mutations of IDH1 in metaphyseal chondromatosis with D-2-hydroxyglutaric aciduria (MC-HGA). *Am J Med Genet Part A.* 2011;155(11):2609-2616.
79. Nota B, Hamilton EM, Sie D, et al. Novel cases of D-2-hydroxyglutaric aciduria with IDH1 or IDH2 mosaic mutations identified by amplicon deep sequencing. *J Med Genet.* 2013;50(11):754-759.
80. Voelker RA, Langley CH, Brown AJ, et al. Enzyme null alleles in natural populations of Drosophila melanogaster: frequencies in a North Carolina population. *Proc Natl Acad Sci USA.* 1980;77(2): 1091-1095.